

An algorithm for modifying neurotransmitter release probability based on pre- and post-synaptic spike timing

Walter Senn^{*,†}, Henry Markram^{*}, and Misha Tsodyks^{*}

^{*} *Department of Neurobiology, The Weizmann Institute, Rehovot 76100, Israel*

[†] *Physiologisches Institut, Universität Bern, Bühlpplatz 5, CH-3012 Bern, Switzerland*

wsenn@iam.unibe.ch, bnmisha@wicc.weizmann.ac.il, bnmark@weizmann.weizmann.ac.il

February 29, 2000

Abstract. The precise times of occurrence of individual pre- and post-synaptic action potentials is known to play a key role in the modification of the synaptic efficacy. Based on stimulation protocols of two synaptically connected neurons, we infer an algorithm which reproduces the experimental data by modifying the probability of vesicle discharge as a function of the relative timing of spikes in the pre- and post-synaptic neurons. The primary feature of this algorithm is an asymmetry with respect to the direction of synaptic modification depending on whether the presynaptic spikes precede or follow the postsynaptic spike. Specifically, if the presynaptic spike occurs up to 50ms before the postsynaptic spike, the probability of vesicle discharge is up-regulated while the probability of vesicle discharge is down-regulated if the presynaptic spike occurs up to 50ms after the postsynaptic spike. In the case where neurons fire irregularly with Poisson spike trains at constant mean firing rates, the probability of vesicle discharge converges towards a characteristic value which is determined by the pre- and post-synaptic firing rates. On the other hand, if the mean rates of the Poisson spike trains slowly change with time our algorithm predicts modifications in the probability of release which generalize Hebbian and BCM rules. We conclude that the proposed spike-based synaptic learning algorithm provides a general framework for regulating neurotransmitter release probability.

Keywords: LTP/LTD, Hebbian learning, release probability, BCM-rule, synaptic depression, neocortex, temporal code

1 Introduction

Since the work of D. Hebb (1949), several attempts were made to formulate precise ‘learning rules’, which could enable one to determine the change in synaptic efficacies from the known activities of neurons (Sejnowski, 1977; Bienenstock et al., 1982; Artola and Singer, 1993; Fregnac and Shulz, 1994). In these rules neuronal activities are represented by an analog variable reflecting the average firing rates of the neurons. Such formulations were used in training neural networks to perform various computational tasks.

Recent experiments indicate that the relative timing of pre- and post-synaptic activity is crucial in determining the magnitude and direction of synaptic modifications (Gustafsson et al., 1987; Fregnac et al., 1988; Stanton and Sejnowski, 1989; Tsumoto, 1990; Debanne

et al., 1995; Bell et al., 1997; Zhang et al., 1998; Bi and Poo, 1998). In particular, Markram et al. (1997) reported that synaptic modification depends on the millisecond relative timing between the pre- and post-synaptic spikes. They found that if presynaptic spikes occur 10 ± 2 ms before the postsynaptic one, then synaptic responses were increased while the same pattern of stimulation with the opposite time delay resulted in a decrease of responses. In addition, in (Markram and Tsodyks, 1996) it was shown that the synaptic modification at this synaptic connection is not a uniform scaling of synaptic strength, but rather a *redistribution* of synaptic efficacy between the spikes in the train. This redistribution of synaptic efficacy can result from the increase in the probability of neurotransmitter release (Tsodyks and Markram, 1997).

The experiments of Markram et al. (1997) provide for the first time the experimental basis for formulating the synaptic learning rules based on individual spikes rather than firing rates. In the current contribution, we present a phenomenological model which reproduces the experimental results and which allows the computation of the synaptic modification for arbitrary patterns of spikes. This model can now be tested against other experimental paradigms and provides a useful foundation for computational models which utilize exact spike timing for information processing (see e.g. Hopfield, 1995). We think that the restriction to the relative spike timing in describing synaptic long-term modifications is a useful simplification which reduces the wealth of possible molecular mechanisms to the functionally relevant behavior of the neurons.

In a second part we investigate the mean-field behavior of our model when applying Poisson spike trains and compare this with existing learning rules based on firing rates. We found that as a function of the postsynaptic activity our rule has a anti-Hebbian and a Hebbian regime similar to the Bienenstock-Cooper-Munro (BCM) rule. It also reproduces a sliding threshold property similar to the BCM theory. Moreover, by setting the synaptic parameters it is possible to generate different types of Hebbian modifications which are either closer to a covariance, a Hebbian or a anti-Hebbian rule. We consider simplifications of our physiologically motivated algorithm and provide a minimal model for an asymmetric spike-based learning rule for the vesicle release probability. Finally, the nonlinearities in our model are put into relation to other spike-based learning rules focusing on aspects of synaptic stability and sensitivity (Abbott and Song, 1999; Kempter et al., 1999b; Kempter et al., 1999a). A short form of the present work is published in Senn et al. (1997).

2 The Model

Our scheme enables the adaptation of the probability of neurotransmitter release resulting from simultaneous activity of pre- and post-synaptic neurons. Specifically, we adapt the probability that a presynaptic spike discharges a vesicle which is ready at the site of release. We refer to this probability as the probability of discharge, P_{dis} . The biophysical processes involved in modifying P_{dis} are triggered either by a postsynaptic spike or by a presynaptic release. Up-regulation of P_{dis} is assumed to be induced by a postsynaptic spike following a presynaptic release. Down-regulation of P_{dis} , on the other hand, is induced by a presynaptic release following a postsynaptic spike.

Practically, long-lasting synaptic modification does not instantaneously follow the pairing but develops slowly to peak 10-20 minutes after the pairing. Accordingly, while implementing the algorithm, P_{dis} is kept fixed and effects of each spike are summed up to determine the overall change in the *limit* probability, denoted as P_{dis}^{∞} . This work does not include a short lasting up-regulation of P_{dis} analogous to post tetanic potentiation because

this phenomenon is not clearly evident at these depressing synapses. Neither considered is any decay of P_{dis}^∞ which could occur on a time scale of hours.

In detail, the synaptic modification works as follows (cf. Fig. 1 and 2). The primary events for up- and down-regulation are mediated by the NMDA-receptors located at the postsynaptic membrane. The following scheme is chosen because both, up- and down-regulation depend on NMDA receptor activation (Markram et al., 1998b, and HM, unpublished results). These receptors may be in 3 different states: the recovered state, N_{rec} , the state saturated with glutamate, N_u , and the state altered by intracellular calcium, N_d . The secondary messenger for up- and down-regulation may be in an active state, S_u and S_d , or in an inactive state, \bar{S}_u and \bar{S}_d , respectively. If a vesicle of neurotransmitter discharges, either spontaneously or due to a presynaptic action potential, glutamate is released and bound by postsynaptic NMDA-receptors ($N_{rec} \rightarrow N_u$). Being in a state saturated by glutamate, the NMDA-receptors will open when the postsynaptic membrane potential increases due to a back-propagating postsynaptic action potential and this induces calcium flowing through NMDA-channels into the postsynaptic cell. This calcium activates a secondary messenger ($\bar{S}_u \rightarrow S_u$) which diffuses to the presynaptic site and up-regulates the probability of discharge ($\bar{P}_{dis}^\infty \rightarrow P_{dis}^\infty$). If, on the other hand, the postsynaptic membrane potential first increases due to a back-propagating action potential, voltage activated calcium-channels open, calcium flows in through these channels and binds to the NMDA-receptors (Mayer et al., 1987), altering or redirecting their function ($N_{rec} \rightarrow N_d$). Subsequently released glutamate which is triggered by a presynaptic action potential now activates an altered NMDA receptor and this leads to the activation of down-regulating secondary messenger ($\bar{S}_d \rightarrow S_d$). This messenger diffuses back to the presynaptic location and the probability of discharge is down-regulated ($P_{dis}^\infty \rightarrow \bar{P}_{dis}^\infty$).

2.1 The algorithm for modifying the discharge probability

The above scenario can be summarized in the following 'learning rule'. Whenever a postsynaptic action potential arrives at the synaptic site, 3 different processes are induced (indicated by *post1* - *post3* in the scheme):

- post1 The fraction r_d^N of N_{rec} is moved to N_d . This describes the altering of NMDA-receptors due to calcium flowing into the postsynaptic site through voltage activated channels.
- post2 The fraction $r^S N_u$ of \bar{S}_u is moved to S_u ($\bar{S}_u = 1 - S_u$). This describes the activation of up-regulating secondary messenger proportional to the amount of-receptors saturated with glutamate.
- post3 The limit probability P_{dis}^∞ is increased by $r_u^P \bar{P}_{dis}^\infty [S_u - S_u^\theta]^+$, where $\bar{P}_{dis}^\infty = 1 - P_{dis}^\infty$ and S_u^θ denotes the threshold to trigger up-regulation ($[x]^+ = \max(x, 0)$). Thus, P_{dis}^∞ is pushed towards 1 proportional to the amount of secondary messenger above threshold.

A release of a vesicle at the presynaptic site induces, completely symmetrically, the following 3 processes (indicated by *rel 1* - *rel 3* in the scheme):

- rel1 The fraction r_u^N of N_{rec} is moved to N_u . This describes the saturation of the recovered NMDA-receptors with glutamate.

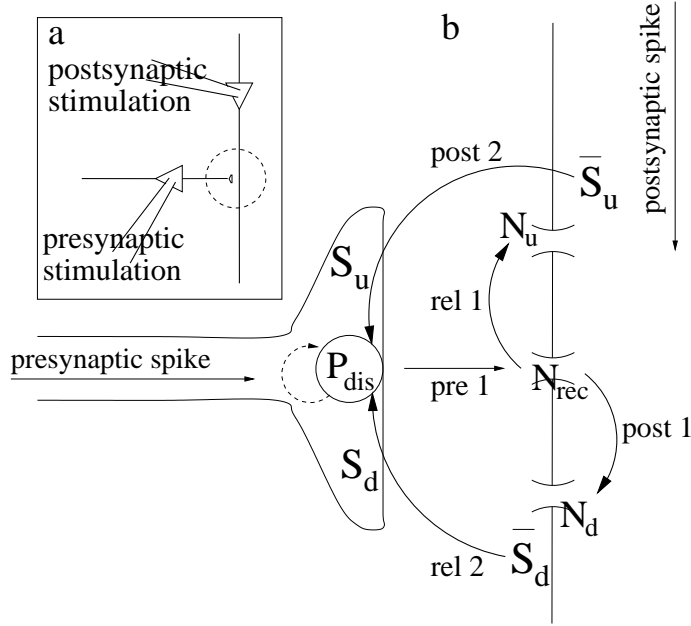


Figure 1: **a** The experimental arrangement. **b** Modification of P_{dis} . A vesicle at the site of release is discharged with probability P_{dis} (arrow pre 1). Up-regulation of P_{dis} requires a presynaptic release (vesicle discharge) followed by a postsynaptic spike (rel 1, post2). Down-regulation requires a postsynaptic spike followed by a presynaptic release (post1, rel 2). N_u and N_d represent NMDA-receptors in the up- and down-regulating state, S_u and S_d represent up- and down-regulating secondary messenger, respectively.

rel2 The fraction $r^S N_d$ of \bar{S}_d is moved to S_d ($\bar{S}_d = 1 - S_d$). This describes the activation of down-regulating secondary messenger proportional to the amount of altered NMDA-receptors.

rel3 The limit discharge probability is reduced by $r_d^P P_{dis}^\infty [S_d - S_d^\theta]^+$, i.e. proportional to P_{dis}^∞ and to the amount of S_d above threshold S_d^θ .

In a temporal order, up- and down-regulation of P_{dis}^∞ are each mediated by a primary and secondary event (cf. scheme): The primary event for up-regulation is a presynaptic release (*rel 1*) and the secondary event is a postsynaptic spike (*post2*). The primary event for down-regulation is a postsynaptic spike (*post1*) and the secondary event is a presynaptic release (*rel 2*).

Beside these instantaneous transitions, the states N_u , N_d and S_u , S_d decay exponentially with the corresponding time constants τ^N and τ^S , respectively. In the diagram, these continuous transitions are represented by the arrows $N_u \xrightarrow{\tau^N} N_{rec}$, $N_d \xrightarrow{\tau^N} N_{rec}$ and $S_u \xrightarrow{\tau^S} \bar{S}_u$, $S_d \xrightarrow{\tau^S} \bar{S}_d$, respectively. The convergence of P_{dis} to the limit probability P_{dis}^∞ evolves with a modification time constant $\tau_M^P = 10$ min. For a formulation of the kinetic scheme in terms of differential equations see Appendix A.1.

2.2 The model of stochastic release

Since on the presynaptic side the algorithm deals with *release* events we modeled their generation by presynaptic *spike* events. This was done by two independent stochastic

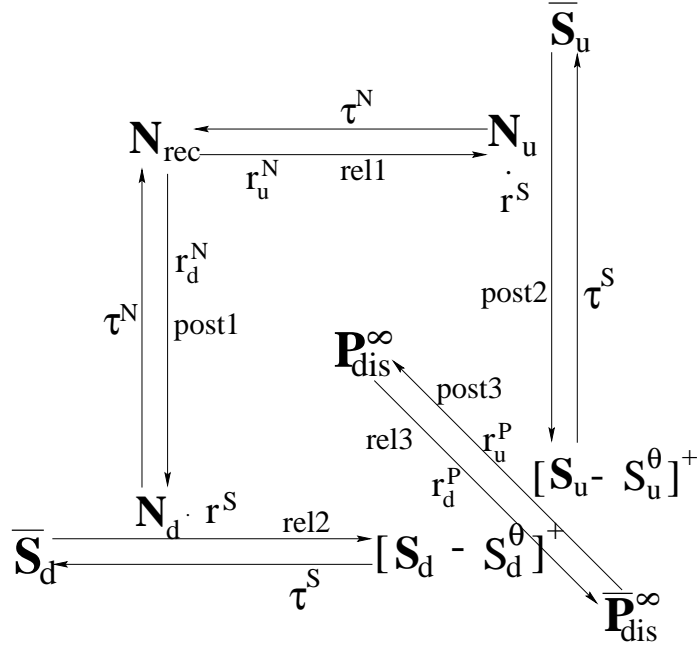


Figure 2: The kinetic scheme for modification of the limit probability of discharge, P_{dis}^∞ . Up-regulation of P_{dis}^∞ is mediated through the states N_u and S_u while down-regulation is mediated through the states N_d and S_d . These states decay naturally with time constants τ^N and τ^S , respectively. Transitions labeled with rel_i and $post_i$ ($i=1,2,3$) occur instantaneously at either a presynaptic release or at a postsynaptic spike. These instantaneous transitions are weighted by the factors written onto their arrows. For instance, at a postsynaptic spike, the state N_d is increased by $N_{rec} \cdot r_d^N$ (post1) and the state S_u is increased by $\bar{S}_u \cdot N_u \cdot r^S$ (post2). At a presynaptic release, for instance, P_{dis}^∞ is decreased by $r_d^P \cdot P_{dis}^\infty \cdot [S_d - S_d^\theta]^+$ (rel 3).

processes. First, a presynaptic action potential arriving at the synaptic bouton discharges a vesicle docked at the site of release with probability P_{dis} . Second, the probability that a vesicle is available at the site of release, P_v , is zero immediately after a vesicle discharge and recovers by a Poisson process with time constant $\tau_v^{rec} \approx 800\text{ms}$, i.e. at any time step there is a small probability (proportional to $1/\tau_{rec}$) that the site of release will be re-occupied by a vesicle. The effective probability of release is given by the joint probability of the two stochastic processes, $P_{rel} = P_{dis}P_v$. Thus, to complete the algorithm, a presynaptic spike induces the following instantaneous transition (denoted by *pre 1* in Fig. 1b):

- pre1 If the site of release is occupied by a vesicle (which occurs with probability P_v) this vesicle is discharged by a presynaptic spike with probability P_{dis} and the site of release is cleared (setting $P_v = 0$).

Note that in accordance to the univesicular hypothesis (Triller and Korn, 1982) we assume that per release site there is maximally one vesicle ready for release. The complete algorithm for synaptic modification and synaptic depression is compiled in a pseudocode in Table 1.

The vesicle depletion model described above is a stochastic version of the depressing synapse model introduced in Tsodyks and Markram (1997). Since the recovery is not instantaneous, a presynaptic spike following a previous discharge has less chance to encounter again a vesicle for discharging and thus in the average the response appears to be depressed.

To decide iteratively whether a presynaptic spike is successful or not we introduce the probability P_{rel}^n that the n -th presynaptic spike induces a release. Note that $P_{rel}^n = P_{dis}P_v^n$ is the product of the vesicle discharge probability and the probability of encountering a docked vesicle at arrival of the n th spike. The probability of release for the $(n + 1)$ -th spike is calculated to (cf. Appendix A.2)

$$P_{rel}^{n+1} = P_{rel}^n(1 - P_{dis})e^{-\frac{\Delta_n}{\tau}} + P_{dis}(1 - e^{-\frac{\Delta_n}{\tau}}), \quad \tau = \tau_v^{rec}, \quad (1)$$

where $\Delta_n = t_{pre}^{sp,n+1} - t_{pre}^{sp,n}$ is the time difference between the two presynaptic spikes and P_{dis} is the current value of the discharge probability. Averaged over different trials with the same stimulation protocol will give an average EPSP amplitude in response to the n -th spike which is proportional to P_{rel}^n . In Tsodyks and Markram (1997) this proportionality constant is called *absolute synaptic efficacy* (A) while, in their mean-field model, the *use of synaptic efficacy* (U) describing the fraction of available transmitter discharged by a presynaptic spike corresponds to our discharge probability P_{dis} . In turn, the probability P_v of a vesicle being docked at the site of release is interpreted as the fraction of transmitter available for release. In the mean-field model the average is taken either over several repetitions of the stimulation frequency, or equivalently, over several release sites in the same or in different boutons for a single sample stimulus. Note that implicitly the univesicular hypothesis (per release site) is assumed since the full amount of discharged transmitter is missing immediately after a presynaptic spike, indicating that after discharge no additional vesicles are ready for release. Our stochastic version may replicate the statistics of the non-averaged responses during single trials of the synaptic stimulation experiments (cf. Tsodyks and Markram, 1997).

3 Results

3.1 Application of specific stimulation protocols

The algorithm is based on dual whole-cell voltage recordings of neocortical pyramidal cells (Markram et al., 1997). It was tested against the following 3 experiments:

Experiment1 (Fig. 3): Pre- and postsynaptic spike trains of 10Hz and 5 spikes were paired with a lag of the presynaptic spikes of -10 and $+10$ ms, respectively, repeated 10 times each 4 seconds. After pairing the change in P_{dis} was recorded during the next 60min. The increase in P_{dis}^∞ for the 10ms advanced presynaptic spikes and the decrease for the 10ms retarded presynaptic spikes was faithfully reproduced by the algorithm. By translating the spike trains such that the last presynaptic spike was 100ms apart of the first postsynaptic spike (and vice versa), no change occurred.

Experiment2 (Fig. 4): Paired pre- and postsynaptic spikes trains of 5 spikes were triggered with a delay of the postsynaptic train of 2 ms, repeated 10 times each 4 seconds. The simulation was performed for different frequencies ranging from 2 to 40Hz and the final change in the probability of discharge, P_{dis}^∞ , is evaluated. The main characteristics of the learning curve, the steep upstroke at 10Hz and the saturation at higher frequencies, are well reproduced.

Experiment3 (Fig. 5): Pre- and post-synaptic spike trains of 20Hz were paired with a postsynaptic spike delay of 2 ms, repeated 10 times each 4 seconds. The number of spikes in the paired trains were varied from 2 up to 20 and for each number P_{dis}^∞ was determined. The surprising fact in this experiment was that the change in P_{dis}^∞ did not accumulate but

```

for t=1 : dt : T
  if postsynaptic spike at t
     $N_d = N_d + r_d^N N_{rec}$ 
     $S_u = S_u + r^S N_u (1 - S_u)$ 
     $P_{dis}^\infty = P_{dis}^\infty + r_u^P [S_u - S_u^\theta]^+ (1 - P_{dis}^\infty)$ 
  end      % end of postsynaptic spike
  if presynaptic spike at t
    if vesicle_docked == 'yes'
      if random  $\leq P_{dis}$ 
        vesicle_docked = 'no'
         $N_u = N_u + r_u^N N_{rec}$ 
         $S_d = S_d + r^S N_d (1 - S_d)$ 
         $P_{dis}^\infty = P_{dis}^\infty - r_d^P [S_d - S_d^\theta]^+ P_{dis}^\infty$ 
      end      % end of vesicle discharge
    end      % end of discharge trial
  end      % end of presynaptic spike
  if random  $\leq \frac{dt}{\tau_{rec}}$ 
    vesicle_docked = 'yes'
  end      % end of vesicle recovery
   $S_u = S_u \exp(-\frac{dt}{\tau^S})$ ,    $S_d = S_d \exp(-\frac{dt}{\tau^S})$ 
   $N_u = N_u \exp(-\frac{dt}{\tau^N})$ ,    $N_d = N_d \exp(-\frac{dt}{\tau^N})$ 
   $N_{rec} = 1 - N_u - N_d$ 
   $P_{dis} = P_{dis} + \frac{dt}{\tau_M} (P_{dis}^\infty - P_{dis})$ 
end      % end of simulation

```

Table 1: Pseudocode for the stochastic synapse with depression together with the kinetic scheme for modifying P_{dis} (Fig. 2). The time step is set to $dt = 1$ ms and the simulation time extents over T ms. The variable ‘random’ represents a random number sampled from the uniform distribution between 0 and 1. The two sets of parameter values are given in the captions to Fig. 3 and Fig. 7.

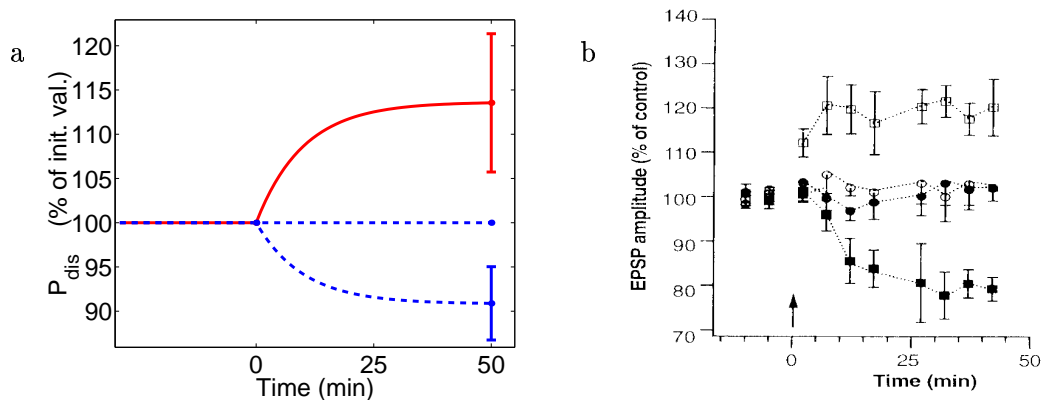


Figure 3: *Experiment1: Asymmetry of the synaptic modification: The evolution of P_{dis} towards P_{dis}^{∞} induced by pairing of 5 spikes at 10Hz with a delay of the presynaptic spike train of $-10ms$ (upper trace) and $10ms$ (lower trace). If the last presynaptic and the first postsynaptic spike were separated by $100ms$ no change occurs (middle traces). **a** Simulation results. The parameter values appearing in the scheme (Fig. 2) were chosen to optimally fit the experimental data. We set $r_u^N = 1, r_d^N = .5, \tau^N = 300ms, r^S = .7, r_u^P = r_d^P = .1$ and $\tau^S = 600ms$. The thresholds for the secondary messengers were set to $S_u^{\theta} = r^S$ and $S_d^{\theta} = r^N r^S$. As starting value for the discharge probabilities we used $P_{dis} = P_{dis}^{\infty} = .5$. **b** The same experiment in the slices. (Reprinted with permission from Markram et al., 1997, Fig. 3C. Copyright 1997 American Association for the Advancement of Science (AAAS).) Note that the change in P_{dis} (as shown in (a)) is proportional to the change in the EPSP amplitude of an isolated spike (as shown in (b), cf. main text). Vertical bars in (a) and (b) represent standard deviations.*

was rather neutralized by the following spikes. The simulations are compatible with these results and lay within the high standard deviations.

The experimental data in Fig. 3-5b show the changes in the amplitude of a first EPSP after a long period of silence. These changes could be induced by a change in either the absolute synaptic strength or the vesicle discharge probability. Inspecting the depression within a spike sequence, however, shows that after pairing synapses with higher amplitude in the first EPSP are also more depressed in the responses to the subsequent spikes (data not shown). The time course of this depression is well predicted by formula (1) with a modified P_{dis} and a fixed proportionality constant. We therefore conclude that it is indeed P_{dis} which is subject to the long-term modification and not the absolute synaptic strength.

What yet has to be tested for the cortical synapses in consideration is the change in P_{dis} for pre- and post-synaptic spike trains of a given frequency and varying delays. In other preparations pairs of single pre- and post-synaptic spikes with frequency 1 Hz and various interspike delays were applied (Zhang et al., 1998; Bi and Poo, 1998). The same protocol applied to our model with parameter values used to fit experiments 1 – 3 yields a change in P_{dis} (Fig. 6a) which looks rather close to the change in the synaptic strength observed in Bi and Poo’s experiments and matches well the width of the modification window. However, the size of the induced changes is much smaller than that seen in their experiment. In our simulation we had to introduce a thresholds precisely to exclude too much up-regulation at a low stimulation frequency (cf. Fig. 3). Cortical synapses seem to be protected against modifications induced by single paired of spikes as long as these pairs do arrive less frequent

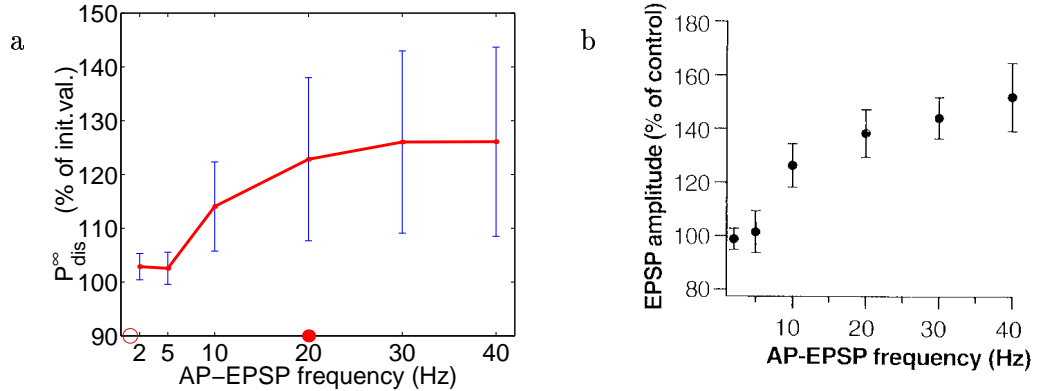


Figure 4: *Experiment2: Dependency on the frequency of the paired spike trains, each composed of 5 spikes. The change in P_{dis} shown 60 minutes after pairing of the spike trains with 2 ms delay of the postsynaptic train. In our model the value of P_{dis} 60 minutes after pairing corresponds to P_{dis}^{∞} (cf. Eq. 14). **a** Simulation results with the same parameter values as in Fig. 3. The value at the dot (20 Hz) and the circle (1 Hz) should be compared with corresponding ones in Fig. 5a and Fig. 6a,b, respectively. **b** Same experiments in the slices. (Reprinted with permission from Markram et al., 1997, Fig. 2C. Copyright 1997 AAAS.)*

than 5 Hz. Such a protection mechanism would make sense in stabilizing memory (Fusi et al., 1999).

If the same number of paired spikes with the same relative delay as in the cited experiment is applied to our cortical synapse model with a frequency higher than 5 Hz a considerable change is evoked. The time constant with which the repetitive stimulations are integrated is determined by the time constant of the secondary messenger τ^S while the width of the learning window itself is determined by the time constant of the NMDA-receptors τ^N , each corrected by the threshold effect. Figure 6b shows the relative change in P_{dis}^{∞} for spike trains of 5 spikes at 20 Hz with different delays of the presynaptic train with respect to the postsynaptic one. The 5 peaks in the upper and lower branch are each due to the partial synchrony induced by a full shift of an interspike interval. For a delay below -200 ms and above $+200$ ms the spike patterns do not interfere anymore and the smoothly decaying branches represent the effective window of modification. Notice that down-regulation is maximal at a delay of 100 ms of the presynaptic spike train while up-regulation is maximal at a delay of -50 ms. The minimum at 100 ms (instead of 1 ms) delay is explained by the fact that at a postsynaptic spike only the fraction r_d^N of N_{rec} is moved to N_d . In turn, the maximum at -50 ms (instead of -1 ms) delay is explained by the fact that not each presynaptic spike induces a neurotransmitter release. The singularity in our simulation at zero delay is an artifact of our simplified model which assumes instantaneous changes in the kinetic scheme. Depending on the true time course of the reactions in the scheme, the singularity will smooth out and the zero change of P_{dis}^{∞} may appear either at a positive or a negative delay.

It is interesting to note that our cortical synapse model would reproduce the same size of the synaptic change as in the cited experiments if not 50 but 500 paired spikes at 1 Hz are applied. The reason is that for frequencies below 5 Hz the induced changes in P_{dis}^{∞} add nearly linearly with the number of paired action potentials. This is not true anymore for a

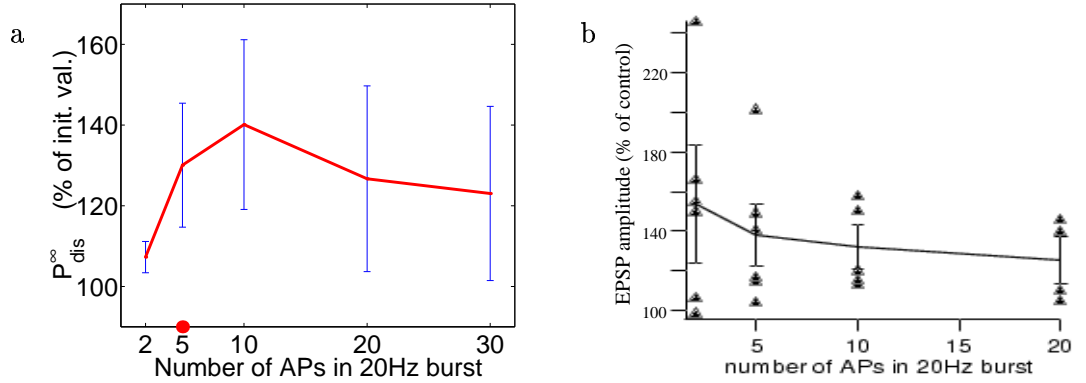


Figure 5: *Experiment3: Dependence on the number of spikes within the paired 20 Hz spike trains. a* Simulation results with the same parameter values as in Fig. 3. *b* Same experiments in the slices. The triangles show the outcome of the experiment with different pairs of cells (2APs: $n=6$; 5APs: $n=6$; 10APs: $n=5$; 20APs: $n=4$; n =number of different pairs).

frequency of 20 Hz as revealed by experiment 3 (cf. Fig. 5).

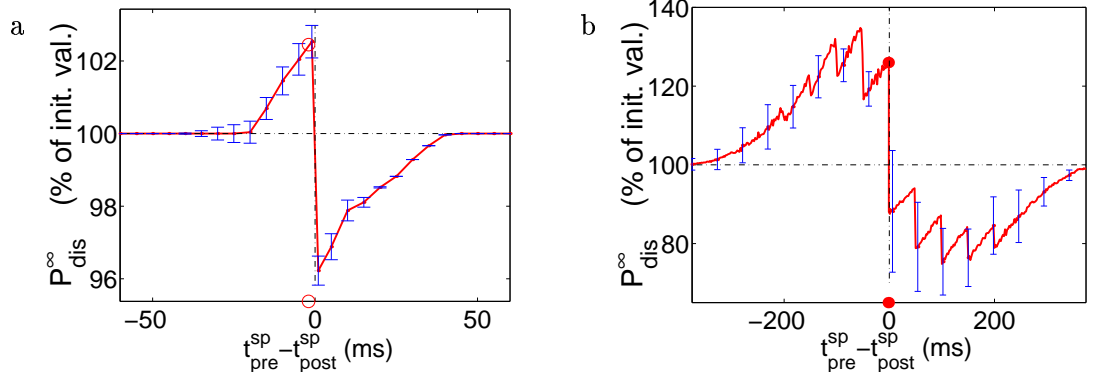


Figure 6: *Change of P_{dis} versus interspike delays ($t_{pre}^{sp} - t_{post}^{sp}$). a* In analogy to the experiment in Zhang et al., 1998, 50 paired spikes at 1 Hz were applied with a fixed presynaptic spike delay between -60 and 60 ms. The curve is qualitatively similar to the experimentally observed one but due to the threshold effect almost no change in P_{dis} is manifested (cf. Fig. 4a,b evaluated at 1 Hz). *b* Pairing with the same number of spikes but now ordered in a 20 Hz train of 5 spikes with a fixed delay of the presynaptic spike train between -350 and 350 ms, repeated 10 times, leads to a marked change in P_{dis} (note the different scales in **a** and **b**). Error bars drawn for selected points only.

3.2 Application of Poisson spike trains

Next we investigate the average behavior of our spike based learning rule when applying non-stationary Poisson spike trains. In this case the kinetic scheme can directly be translated into differential equations with time-varying coefficients. Following the diagonal arrows in the scheme, P_{dis}^{∞} is up-regulated at each postsynaptic spike proportionally to $(1 - P_{dis}^{\infty}) [S_u - S_u^{\theta}]^+$ and down-regulated at each presynaptic release proportionally to $P_{dis}^{\infty} [S_d - S_d^{\theta}]^+$, where $[x]^+ = \max\{x, 0\}$. If we denote the presynaptic release and postsynaptic spike frequency

by f_{pre}^{rel} and f_{post}^{sp} , respectively, the expected change of P_{dis}^∞ at time t is obtained from the kinetic scheme according to

$$\frac{dP_{dis}^\infty}{dt} = r_u^P (1 - P_{dis}^\infty) [S_u^+ - S_u^\theta]^+ f_{post}^{sp} - r_d^P P_{dis}^\infty [S_d^+ - S_d^\theta]^+ f_{pre}^{rel}, \quad (2)$$

where S_u^+ and S_d^+ represent the expectation values of the secondary messengers for up- and down-regulation immediately after a post- and pre-synaptic spike, respectively (cf. Appendices A.1-A.3). Such an expectation value corresponds to the average over a population of identical synapses with the same instantaneous spike statistics. If the secondary messengers has a time constant large enough to integrate the signals it will be itself roughly proportional to the first-order correlation $f_{pre}^{rel} f_{post}^{sp}$. Neglecting the thresholds S^θ , the first term in (2) then is of order $f_{pre}^{rel} (f_{post}^{sp})^2$ while the second term is of order $f_{post}^{sp} (f_{pre}^{rel})^2$. It is this higher-order nonlinearity which keeps the synapse sensitive not only to spike correlations, but also to average firing rates. For stationary Poisson trains P_{dis}^∞ converges to a unique steady state (see Fig. 7a and Eq. (23) in Appendix A.3) which is increasing with respect to f_{post}^{sp} and weakly decreasing with respect to f_{pre}^{sp} and f_{pre}^{rel} , respectively (Fig. 7b). In this section we preferred to choose a simpler parameter setting with vanishing thresholds and which is symmetric with the exception of the rates for up- and down-regulation. In order to obtain the anti-Hebbian regime at low postsynaptic frequencies in the BCM-rule a high ratio $\frac{r_d^P}{r_u^P}$ is necessary.

In the following we modulate the Poisson spike frequencies and impose additional spike-by-spike correlations. We consider 3 scenarios each of which reveals a particular aspect of our learning rule: A) A jump in the postsynaptic spike frequency leads to an adaptation of P_{dis}^∞ similar to the synaptic weight adaptation in the BCM-theory. B) Modulating sinusoidally the pre- and post-synaptic frequencies with a fixed phase lag leads to an adaptation of P_{dis}^∞ reminiscent to a Hebbian/anti-Hebbian rule. C) Introducing spike-by-spike correlations within the pre- and post-synaptic spike trains (while keeping their frequencies fixed) leads to an adaptation of P_{dis}^∞ depending on the relative spike timing.

A) Comparison with the BCM-rule

The theory of Bienenstock, Cooper and Munro (BCM) (Bienenstock et al., 1982) was developed to explain the synaptic modifications in the visual cortex of cats observed under various rearing conditions (for a review see Bear et al., 1987). In the monocular deprivation experiment a cortical cell which initially dominantly responded to the deprived eye is shown to slowly shift its dominance to the untouched eye. In BCM-theory this is explained by a sliding threshold for the postsynaptic activity, θ_M , which determines whether the synaptic strengths are down- or up-regulated. After suturing the dominant eye the preferred stimulus may only sub-critically excite the postsynaptic cell and the strengths of the activated synapses are down-regulated. To gain the sensitivity to an activity pattern from the unsutured eye the modification threshold θ_M slowly decays until the postsynaptic activity becomes super-critically and the synapses from the untouched eye are now strengthened and finally dominate the cell's firing behavior. In our context, the synaptic modification may be written as

$$\frac{dP_{dis}^\infty}{dt} = r_u^P \phi(f_{post}^{sp}) f_{pre}^{rel}, \quad (3)$$

where ϕ , as a function of the postsynaptic activity, satisfies the BCM-properties $\phi(0) = \phi(\theta_M) = 0$ and $\phi(f_{post}^{sp}) \leq 0$ if $f_{post}^{sp} \leq \theta_M$ and $\phi(f_{post}^{sp}) > 0$ if $f_{post}^{sp} > \theta_M$ (see Fig. 8b).

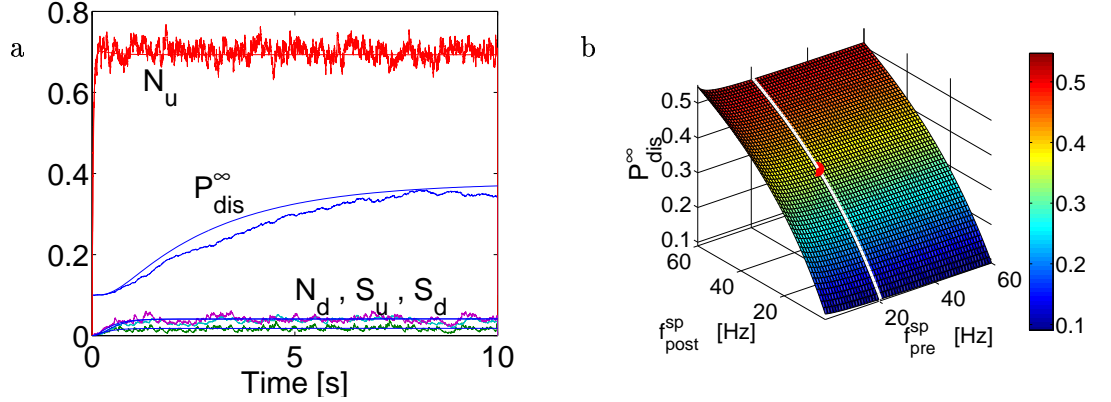


Figure 7: **a** The convergence to the steady states of N_u , N_d , S_u , S_d and P_{dis}^∞ from the starting values 0 and 0.1, respectively. The applied Poisson frequencies were fixed to $f_{pre}^{sp} = 20$ and $f_{post}^{sp} = 30$ Hz. The noisy curves represent an average over 100 trials (of the algorithm in Table 1) while the smooth lines represent the mean field solutions (obtained by integrating the differential equations (8) - (15)). **b** For each pre- and post-synaptic Poisson spike frequency there is a unique steady state for $P_{dis}^\infty = P_{dis}$ (plot of (23) in Appendix A.3). The sensitivity to f_{post}^{sp} is mainly due to the higher order term in f_{post}^{sp} while the insensitivity to f_{pre}^{sp} is due to the synaptic depression. The white curve shows P_{dis}^∞ restricted to $f_{pre}^{sp} = 20$ Hz and the dot on this curve corresponds to $f_{post}^{sp} = 30$ Hz with a discharge probability of $P_{dis}^\infty \approx 0.37$ (cf. left panel). The insensitivity in f_{pre}^{sp} is explained by the synaptic depression while the sensitivity in f_{post}^{sp} is mainly due to the higher order term in f_{post}^{sp} . The parameters were $\tau_u^N = \tau_d^N = 100$ ms, $\tau_u^S = \tau_d^S = 800$ ms, $r_u^N = r_d^N = .8$, $r^S = .4$, $r_u^P = .1$, $r_d^P = 1$, $S_u^\theta = S_d^\theta = 0$.

Note that unlike to the BCM-theory where the ϕ is only a function of the postsynaptic rate it depends on the individual synapse in our case. Distinguishing between the f_{post} -dependency of ϕ on a fast and slow time scale leads to the sliding threshold property. Taking into account the transfer from the presynaptic frequencies to the postsynaptic response, this is an important means of the synapses to keep the postsynaptic activity around a point of the cell's maximal sensitivity. If e.g. after reaching steady state values the postsynaptic frequency drops, say by artificially reducing the input from the dominant eye, P_{dis}^∞ of the activated synapses is slowly down-regulated (Fig. 8a). The rate of the change in P_{dis}^∞ and its final value are shown in Fig. 8b as a function of the new value of f_{post}^{sp} . The modulation threshold θ_M at which up- and down-regulating forces neutralize is implicitly driven by the running mean of the postsynaptic spike frequency: keeping the spike frequencies fixed at the new value, the synaptic parameters will adapt such that f_{post}^{sp} becomes a zero of ϕ and therefore $\theta_M = f_{post}^{sp}$ (cf. Appendix A.4 for an analytical treatment). At this point a slight change in the postsynaptic average frequency will result in a corresponding change of the vesicle discharge probability. A new presynaptic activation pattern, say generated by stimulating the unsutured eye, sharing the same synapses will now have the chance for growing influence onto the postsynaptic cell and the average postsynaptic activity would again start to increase. A more detailed discussion of the learning rule's selection and stabilization properties to dominant input patterns is given in (Kempster et al., 1999b; Abbott and Song, 1999). Let us finally mention that it is possible to retrieve the rule of Artola-Bröcker-Singer (Artola and Singer, 1993) which differs from the BCM rule by

an additional threshold below which no modification takes place. In our scheme this is achieved by setting both thresholds S_u^θ and S_d^θ to positive values.

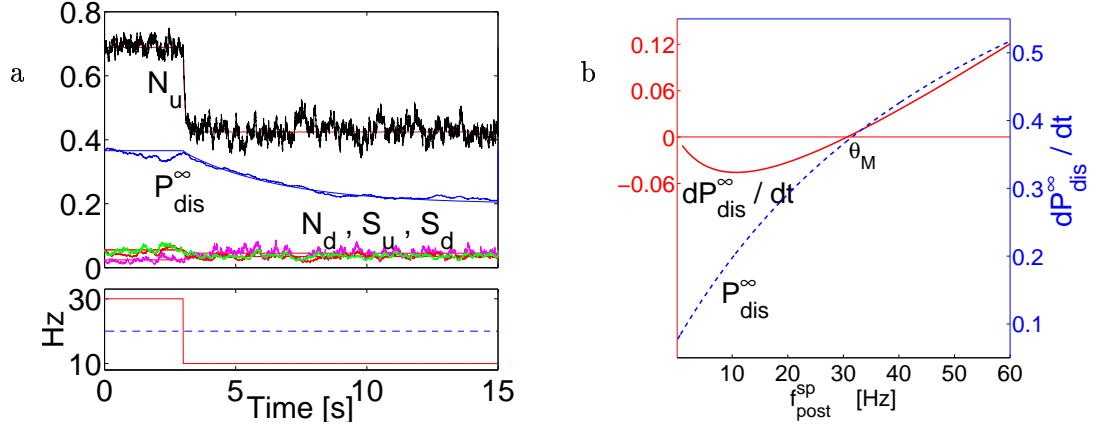


Figure 8: *The BCM rule. a* After converging to the steady state for $f_{pre}^{sp} = 20$ and $f_{post}^{sp} = 30$ Hz, an instantaneous jump of the postsynaptic frequency to 10Hz will down-regulate P_{dis}^∞ . Noisy lines represent the average over 50 trials (of the algorithm in Table 1) while the smooth lines represent the mean field solutions (obtained by integrating the differential equations (8) - (15)). *b* Starting at the same steady state as in (a) the vesicle discharge probability increases if the postsynaptic spike frequency jumps above θ_M ($= 30$ Hz) and decreases if it jumps below. The rate of the change is a non-monotonic function of the new value of f_{post}^{sp} (solid line, calculated according to (3) and Appendix A.4 with $f_{pre}^{sp} = 20$ Hz). The dashed curve shows the new value of P_{dis}^∞ after reaching the steady state and corresponds to the white curve in Fig. 7b.

B) A generalized asymmetric Hebbian rule

Different forms of Hebbian learning rules have been investigated in recent years which consider the product of pre- and post-synaptic activities as the quantity determining the synaptic modification (see e.g. Brown and Chatterji, 1994, for a review). To prevent the saturation of the synaptic strengths mixtures of Hebbian and anti-Hebbian rules are proposed by focusing on the covariance between pre- and post-synaptic activities (Sejnowski, 1977) or by normalization of the synaptic weight (Oja, 1982). The learning rule we consider belongs to the same class of Hebbian mixtures, however, with a strong asymmetry in the temporal correlations. This asymmetry makes the synapse sensitive to the phase lag between modulations of the pre- and post-synaptic frequencies: if the postsynaptic spike activity lags the presynaptic release activity, P_{dis}^∞ is up-regulated and if the postsynaptic spike activity leads the presynaptic release activity, P_{dis}^∞ is down-regulated. Figure 9a shows the change of P_{dis}^∞ for a sinusoidal modulation of the pre- and postsynaptic spike frequencies of 1Hz and phase lag of 0.2. The steady state of P_{dis}^∞ for different rates of modulation and different lags is shown in Figure 9b. Two things are worth emphasizing. First, for slow modulation rates in the range of the vesicle recovery time constant the point of zero change appears at positive lag of the presynaptic activity. This is rather counter-intuitive since at positive lag down-regulation would be expected. Second, the maximal changes appear at lags of $\pm \frac{1}{4}$ independently of frequency of modulation. This is even true if the period of the modulation is much larger than the time window of synaptic adaptation.

To gain insight into these mechanisms we constrain ourselves to the simplifying assumption of an instantaneous recovery of the secondary messenger ($\tau^S = 0$). This assumption implies that the amount of activated secondary messenger S_u and S_d is always proportional to the NMDA receptors in the states N_u and N_d , respectively. On the other hand, if the pre- and post-synaptic spikes are independent, these states are roughly proportional to the running mean of the previous presynaptic release and postsynaptic spike frequencies, respectively (which follows from integrating (8) and (9) in A.1). If we moreover neglect the thresholds for up- and down-regulation ($S_u^\theta = S_d^\theta = 0$), then formula (2) for the synaptic modification can be comprised by the generalized asymmetric Hebbian rule

$$\frac{dP_{dis}^\infty}{dt} \approx r_u^P (1 - P_{dis}^\infty) \langle f_{pre}^{rel} \rangle f_{post}^{sp} - r_d^P P_{dis}^\infty \langle f_{post}^{sp} \rangle f_{pre}^{rel}, \quad (4)$$

where

$$\langle f \rangle = \frac{1}{\tau^N} \int_0^\infty f(t - t') e^{-t'/\tau^N} dt'$$

represents the running mean of f . Note that by the setting $\tau^S = 0$ the third-order non-linearity in (2) is reduced to the usual correlations, although with the presynaptic release instead of the presynaptic spike frequency. The transformation of the presynaptic spike to the presynaptic release frequency itself is governed by the dynamics of the vesicle recovery (cf. Eqs 15 and 16). If we assume an instantaneous vesicle recovery ($\tau_v^{rec} = 0$), there is no activity dependent depression and the presynaptic *release* rate is proportional to the presynaptic *spike* rate. For ‘static’ synapses f_{pre}^{rel} can therefore be replaced by f_{pre}^{sp} in (4).

The above equation provides an explanation of Figure 9. First, we observe that averaging f over the past delays the averaged quantity $\langle f \rangle$. Second, we note that the effect of the synaptic depression is to advance the release rate f_{pre}^{rel} compared to the spike rate f_{pre}^{sp} (since the peak of the release rate is depressed, see e.g. (Abbott et al., 1997)). For lag zero and a modulation frequency of $\omega = 1$ Hz these two effects cancel and the factors in the Hebbian part of (4) are correlated, but not the ones in the anti-Hebbian part. This explains the up-regulation of P_{dis} even at small positive lag of the presynaptic spike activity (Fig. 9b). For higher modulation frequencies beyond the time constant of vesicle recovery, however, the phase advance vanishes and at zero lag the Hebbian and anti-Hebbian part in (4) cancel each other. The maximal up-regulation is reached for a presynaptic phase advance of $\frac{1}{4}$ since due to the delaying effect of averaging this leads to correlated factors in the Hebbian part of (4) and to uncorrelated factors in the anti-Hebbian part. Similarly, maximal down-regulation of P_{dis} is obtained around a presynaptic phase lag of $-\frac{1}{4}$ and this barely depends on the modulation frequency.

C) A spike correlation rule

In the previous paragraph we considered correlations between pre- and postsynaptic mean firing rates. Independently of these correlations, the pre- and postsynaptic spike trains may exhibit spike-by-spike correlations which affect the synaptic efficacy as well. To quantify the influence of this ‘micro’-correlation we introduce the notion of (*first order*) *spike correlation* between pre- and post-synaptic spike train. This measure describes the temporal asymmetry with which on the average a presynaptic spike occurs between the last previous and the next following postsynaptic spike. For a given presynaptic spike time t_{pre} we denote the time of the previous postsynaptic spike by $t_{post}^<$ and the time of the following

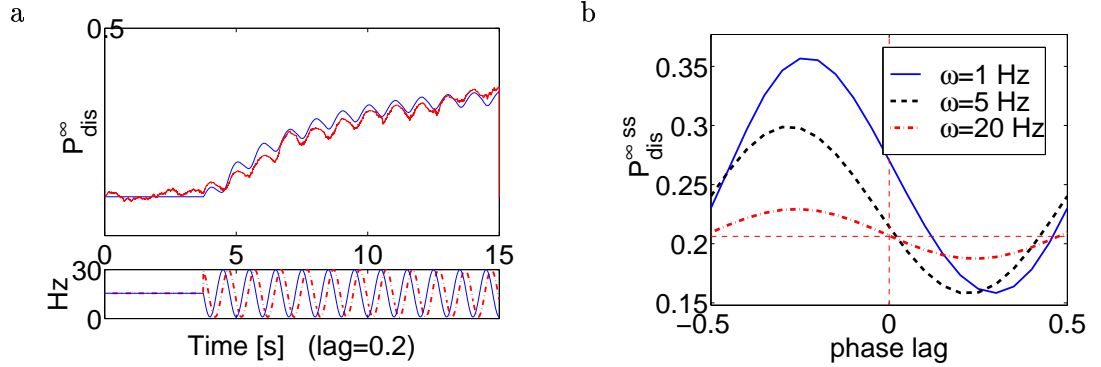


Figure 9: **a** A sinusoidal modulation of f_{pre}^{sp} (full line in the lower panel) and f_{post}^{sp} (dashed line in the lower panel) of $\omega = 1$ Hz with presynaptic phase lag of 0.2 induces up-regulation of P_{dis}^{∞} (upper panel). The noisy line in the upper panel represents the average time evolution of P_{dis}^{∞} over 100 trials (of the algorithm in Table 1) and the dashed curve represents the mean field solution (of Eqs. (8) - (15)). **b** Steady state values of P_{dis} for sinusoidal modulations of the pre- and post-synaptic frequencies versus the presynaptic phase lag. The modulation frequencies where $\omega = 1, 5, 20$ Hz. Note that the curves represent smoothed versions of the learning curves shown in Fig. 6. For the 1 Hz modulation the synaptic depression may advance the release activity with respect to the presynaptic spike activity and P_{dis}^{∞} may be up-regulated even if this lags the postsynaptic peak activity. The horizontal dashed line represents the steady state without modulation. Same parameter values as in the caption of Fig. 7.

postsynaptic spike by $t_{post}^>$. The spike correlation c_s is then defined by

$$c_s := \frac{1}{\Delta} \left(\langle t_{pre} - t_{post}^< \rangle_{t_{pre}} - \langle t_{post}^> - t_{pre} \rangle_{t_{pre}} \right),$$

with normalization $\Delta = \langle t_{pre} - t_{post}^< \rangle_{t_{pre}} + \langle t_{post}^> - t_{pre} \rangle_{t_{pre}}$. Due to the normalization, c_s is restricted to values between -1 and 1 and these boundary values are reached if the presynaptic spikes all occur either instantaneously after or before the postsynaptic ones, respectively. Hence, we characterize the pre- and post-synaptic spike trains by three numbers, their (instantaneous) frequencies and their spike correlation, f_{pre}^{sp} , f_{post}^{sp} and c_s . Although there is no surprise that the sign of the synaptic change will correspond to the sign of the correlation c_s imposed to the spike trains, it is important on a formal level to quantify the synaptic modification as a function of these three variables. The computational power of rate-based neurons with transfer functions depending on the presynaptic correlations was recently characterized (Maass, 1998) but learning algorithms for such networks have yet to be studied.

Let us now assume a scenario where the pre- and post-synaptic spike trains each exhibit Poisson characteristics when considered by themselves but when compared to each other they show some spike correlation $c_s \in [-1, 1]$. Figure 10a depicts the change of P_{dis}^{∞} when after 2 seconds of Poisson stimulation the spike correlation c_s jumps from 0 to 1 (first pre then post) and from 0 to -1 (first post then pre), respectively. Figure 10b shows the steady state of P_{dis}^{∞} as a function of c_s for fixed pre- and post-synaptic frequencies. Re-ordering the left and right branches (inset of the Figure) yields an average modification similar to the one induced by the shift between the periodic pre- and post-synaptic spike trains in Fig. 6.

To explain the effect of the spike correlation we again assume the simplified setting of an instantaneous recovery of the secondary messenger ($\tau^S = 0$) and of vanishing thresholds S_u^θ and S_d^θ . The spike correlation implicitly determines the distribution of the NMDA-receptors over the states N_{rec} , N_u and N_d . If c_s is negative, the transition $N_{rec} \rightarrow N_u$ induced by a presynaptic release is less effective since with high probability an immediately preceding transition $N_{rec} \rightarrow N_d$ induced by a postsynaptic spike reduced the state N_{rec} . Since N_u tunes through the postsynaptic frequency the up-regulation of P_{dis}^∞ , the net increase of P_{dis}^∞ is reduced. In turn, a positive c_s unfavors the state N_d since a previously arrived presynaptic spike triggered with probability P_{rel} the transition $N_{rec} \rightarrow N_u$ and less is remaining in the state N_{rec} to be moved to N_d . In this case the down-regulation of P_{dis}^∞ is less effective. This reasoning can be expressed by adapting formula (4) to

$$\frac{dP_{dis}^\infty}{dt} \approx r_u^P (1 - P_{dis}^\infty) (f_{pre}^{rel} (1 - r_d^N [-c_s]^+)) f_{post}^{sp} - r_d^P P_{dis}^\infty (f_{post}^{sp} (1 - r_u^N [c_s]^+ P_{rel})) f_{pre}^{rel}. \quad (5)$$

Note again that the presynaptic release frequency corresponds to the presynaptic spike frequency times the probability of vesicle release, $f_{pre}^{rel} = f_{pre}^{sp} P_{rel}$, and that the latter itself depends on the dynamics of the presynaptic spike frequency (see (1) and Appendix A.2). Equations (4) and (5) represent an asymmetric version of the traditional covariance rule based on mean firing rates (see e.g. Sejnowski, 1977) with an account of correlations on the level of spikes rather than only on the level of the frequencies.

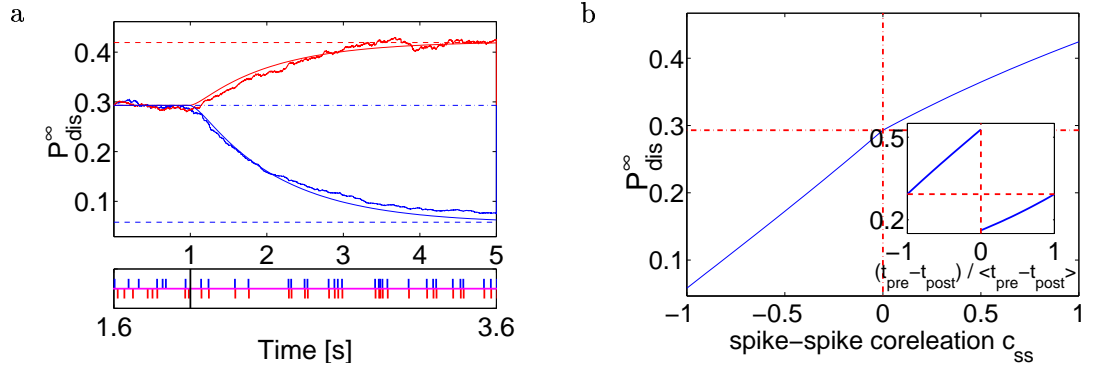


Figure 10: **a** Upper panel: After reaching the steady state for a pre- and post-synaptic Poisson spike train of 20Hz (0 – 2sec) the spike correlation c_s was switched either from 0 to 1 (inducing an increase of P_{dis}^∞) or from 0 to -1 (inducing a decrease of P_{dis}^∞). The noisy lines represent the average for 100 repetitions of the experiment and the smooth lines represent empirically corrected mean field calculations (cf. Appendix A.5). Lower panel: After switching c_s from 0 to 1 the spikes of the postsynaptic neuron (lower trace) were elicited immediately after a presynaptic spike (upper trace). **b** The change of P_{dis}^∞ according to (5) for $f_{pre}^{sp} = 20\text{Hz}$ and $f_{post}^{sp} = 30\text{Hz}$ versus the spike correlations c_s . The inset shows a reordering of the branches and essentially reflects the steady state of P_{dis}^∞ as a function of the (normalized and averaged) spike time differences $t_{pre}^{sp} - t_{post}^{sp}$. Same parameter values as in the caption of Fig. 7.

3.3 Full versus simplified model

One may ask whether the simplified model explaining the mean-field properties in B) and C) above is sufficient to reproduce the experimental results. As long as one is interested in

modeling the temporal asymmetry of the synaptic modification this is indeed true, but it is difficult to fit the nonlinearities of the additional experiments. To recapitulate, the simplified model is obtained by neglecting the dynamics of the secondary messenger, formally by taking the limit $\tau^S = 0$ with $r^S = 1$. (In this case one may simply skip the steps *post2* and *rel2* in the algorithm and directly use the quantities N_u , N_d for S_u , S_d in the steps *post3* and *rel3*, respectively. Similarly, in the mean-field description (2) one may identify S_u^+ , S_d^+ with N_u , N_d , respectively (see Appendix A.3).) In a rough simplification, the discharge probability is then up-regulated at each postsynaptic spike depending on the running mean of the presynaptic release rate and down-regulated at each presynaptic release depending on the running mean of the postsynaptic spike rate,

$$\Delta P_{dis} \approx \langle f_{pre}^{rel} \rangle f_{post}^{sp} - \langle f_{post}^{sp} \rangle f_{pre}^{rel} . \quad (6)$$

This form of the algorithm would represent the minimal model to reproduce the temporal asymmetries in the Figures 3, 6 and 10a, but also in Figure 9b reflecting the phase-advance property of depressing synapses. If the rule is applied to the strength of non-depressing synapses it would probably also be sufficient to reproduce the experiments in other preparations which were confined to investigate the asymmetry of the learning window at a fixed frequency of the pairing (Bell et al., 1997; Zhang et al., 1998; Bi and Poo, 1998). In our case of depressing synapses, however, we did not to succeed to match at the same time the additional experiments 2 and 3 with their nonlinear increase as a function of the pairing frequency and the non-monotonic change as a function of the number of spikes. These two experiments let us introduce the S -variable in the kinetic scheme as well as the third-order nonlinearity given by the steps *post3* and *rel3* (which are established by the delta-function in Eq. 12).

First, two different time constants are needed to model: (1) the width of the learning window which is probably narrower than 50ms as seen in Fig. 3 and 6a; (2) the cumulating effect of the spike pairing repeated in steps of 100ms as shown by the steep increase at 10 Hz in Fig. 4. Experiment 3 also suggests that a time constant larger than 50 ms is involved since a transient behavior is seen extending over the 500ms of the first 10 – 15 spikes of a 20 Hz (see Fig. 5). The choice of two different secondary messengers was guided by the simplicity of the resulting scheme and we do not make any statement about their nature. In fact, one could think of a single type of secondary messenger, but in this case additional processes have to be modeled to read out from this messenger whether and how much the discharge probability should be up- or down-regulated (Grzywacz and Burgi, 1998).

Second, we introduced the third-order nonlinearity since in the presence of synaptic depression it was difficult to obtain a nonlinear increase of the learning curve with respect to increasing frequencies (Fig. 4). The reason is that increasing the pairing frequency is essentially balanced out on the RHS of (6). If we consider the full scheme with large τ^S (compared to $1/f$), however, (6) turns into

$$\Delta P_{dis} \approx \langle f_{pre}^{rel} \rangle_N \langle f_{post}^{sp} \rangle_S f_{post}^{sp} - \langle f_{post}^{sp} \rangle_N \langle f_{pre}^{rel} \rangle_S f_{pre}^{rel} , \quad (7)$$

where $\langle \cdot \rangle_N$ and $\langle \cdot \rangle_S$ denote the running mean with time constants τ^N and τ^S , respectively (cf. (4) and Appendix A.3). Now f_{post}^{sp} arises in the square in the first term which gives the steep increase with the pairing frequency. Importantly, f_{pre}^{rel} which arises in the square in the second term remains in the order of 1 Hz due to the synaptic depression (cf. Appendix A.2). Although this reasoning deals with Poisson rates, the problem that the synaptic change is largely indifferent to increasing frequencies if we wouldn't introduce further nonlinearities

is also seen in experiment 2: At medium frequencies, in a train of 5 paired spikes one of the first and often the last presynaptic spike only triggers a release. In this case the postsynaptic spikes in the middle of the train are placed symmetrically after and before a presynaptic release and no clear dominance for up-regulation is shown. For higher frequencies, the duration of the 5-spike train is markedly below the vesicle recovery time constant and maximally one release can be triggered. Due to the stochastic nature this release may arise in response to the second presynaptic spike and by the preceded postsynaptic event down-regulation is favored. Moreover, since in this case the first postsynaptic spike depleted the common pool (N_{rec}) the same release event will be much less effective in inducing an up-regulation via immediately following postsynaptic spike.

4 Discussion

Summary We presented an algorithm that allows the prediction of the change in the temporal dynamics of synaptic transmission by depressing synapses induced by arbitrary trains of pre- and post-synaptic action potentials. The algorithm is based on the importance of precise relative timing of the pre- and post-synaptic action potentials and therefore constitutes a novel form of learning algorithm. It reproduces the change in the synaptic responses induced by the pairing: the asymmetry with respect to the spike-time difference, the monotonic increase with respect to the frequency and the non-monotonic dependency on the number of paired spikes.

When applying Poisson spike trains, an anti-Hebbian regime is followed by a Hebbian regime during an increase of the postsynaptic frequency, provided the relative degree of up-regulation (r_u^P/r_d^P) is small enough. This feature together with the slow adaptation of the borderline between the two regimes allows the rule to preserve the stability and the selectivity to new patterns as described by the BCM-theory. When modulating the pre- and post-synaptic spike frequencies the synaptic dynamics may dominate the temporal asymmetry of the learning rule and, surprisingly, up-regulation of the discharge probability may occur even if the presynaptic peak activity lags the postsynaptic peak activity. Finally, quantifying the spike correlation within two arbitrary spike trains permits to specify the learning rule as a function of the instantaneous pre- and post-synaptic frequencies and their instantaneous spike correlation. Such a formulation fits into the recently proposed framework of generalized neural networks which are processing average firing rate together with average spike correlations (Maass, 1998).

Experimental basis for the model The algorithm was constructed under several experimental constraints: [1] Excitatory glutamatergic synapses between pyramidal neurons in the neocortex are fast depressing synapses and the change that follows Hebbian pairing is equivalent to a change in the discharge probability P_{dis} (Markram and Tsodyks, 1996). This change alters the temporal dynamics of transmission (Tsodyks and Markram, 1997; Abbott et al., 1997); [2] The asymmetrical modification window with respect to relative timing of pre and postsynaptic action potentials as reported by (Markram et al., 1997) was considered. In this window, up- and down-regulation falls in a window of around 100ms after and before a postsynaptic action potential, respectively; [3] Up regulation is dependent on NMDA receptors and the backpropagating action potential can cause rapid pulses of Ca^{2+} through the NMDA receptor (Markram et al., 1998b; Spruston et al., 1995). The speed of these AP-evoked $[Ca^{2+}]$ pulses via NMDA receptors are such that only an enzyme with very high forward binding rates could capture this Ca^{2+} providing the ideal

situation for a coincident detector protein (Markram et al., 1998b). We therefore propose that the amplitude of the up-regulation follows a time course of the NMDA current which has a rise time constant of 10-20ms and a decay time constant of 100-300ms (Jonas and Spruston, 1994). The time constant of approximately 60ms for up-regulation observed experimentally could be due to a threshold effect; [4] The magnitude of the up-regulation increases as a function of the frequency of the pre and postsynaptic action potentials in the train with an onset between 5 and 10Hz (Markram et al., 1997); [5] Surprisingly, the up-regulation was not increased when more action potentials were included in a train of a given frequency (data included in this study). This is proposed to be due to the balanced effects of up- and down-regulation which, after an initial transient, is reached for the given train of action potentials; [6] Down-regulation is also dependent on NMDA receptor activation and on Ca^{2+} influx (HM, unpublished data). We therefore propose that the rise in the Ca^{2+} -concentration following a back-propagating action potential influences the NMDA receptor in such a manner that it results in down-regulation when activated. Indeed, the dendritic Ca^{2+} transient has a similar time course as that of down regulation (Markram et al., 1995) and intracellular Ca^{2+} has been shown to modify the kinetics of the NMDA receptor (Mayer et al., 1987; Medina et al., 1996; Mayer, 1998; Antonov et al., 1998). [7] Ca^{2+} from different sources or modes of influx can activate different processes due to differential binding as a function of forward and backward rate constants (Markram et al., 1998b).

Comparison with other learning rules Asymmetric learning rules based on mean firing rates or individual spike times were investigated in different contexts. They were used for storing trajectories (Abbott, 1996), for modeling hippocampal place fields of rats wandering around in the Morris water maze (Blum and Abbott, 1996; Gerstner and Abbott, 1997) and for modeling the temporal selectivity in the auditory pathway of barn owls (Gerstner et al., 1996). Recent works investigate the stabilization capabilities of asymmetric rules in keeping the cell's sensitivity (Kempster et al., 1999b; Abbott and Song, 1999), similarly as it is achieved by the described sliding threshold property on the level of mean firing rates. Neither of these works, however, take into account the synaptic dynamics.

The present algorithm comes closest to the version of the learning rule outlined in Gerstner et al. (1998, Sect. 14.2.4) which deals with the kinetics of 4 different components corresponding to our N_u , N_d , S_u and S_d . In their description, again, no synaptic depression is taken into account and the rule refers to a change in the absolute synaptic strength. Moreover, no common pool similar to N_{rec} is assumed and Hebbian second-order correlations are only considered. It is worth pointing out that the physiologically motivated restriction to a common pool N_{rec} may help to sharpen the distinction between positive and negative spike delays, even in the case of a deterministic release without depression: considering simultaneous bursts of pre- and post-synaptic spikes of mixed temporal correlations it would typically be the first release-spike pair which, due to the depletion of the common pool, dominates the synaptic modification. An immediately following second pair with possible reversed temporal order will be much less effective if this pool was just reduced and therefore will not be able to annihilate the initiated modification.

In comparison to rules based on mean-firing rates one may establish connections to the BCM-theory (Bienenstock et al., 1982) but also reproduce the rule of Artola-Bröcker-Singer (Artola and Singer, 1993) by assuming non-vanishing thresholds for the up- and down-regulation. On the other hand, the simplified form (6) shows that the present algorithm is distinct from the covariance rule (Sejnowski, 1977) which in our situation would be of the

form

$$\Delta P_{dis} \approx (f_{pre}^{rel} - \langle f_{pre}^{rel} \rangle) (f_{post}^{sp} - \langle f_{post}^{sp} \rangle),$$

and therefore would be symmetric with respect to the presynaptic release and the post-synaptic spike frequencies. The power of the present algorithm is to cope not only with average firing frequencies and correlations but to offer a general framework for dealing with any pre- and post-synaptic spike train of any complexity and arbitrary correlations.

Predictions of the model and outlook It is remarkable that simple first order kinetics with a cross-gating of the NMDA receptors can qualitatively explain the different spike induced nonlinear synaptic modifications. Several features of the model are tailored to explain the specific experimental results and raise new hypotheses which can be experimentally tested. Among these are: [1] Experiment 2 with a reversed relative timing would lead to a moderate monotonic decrease of P_{dis} with respect to the paired spike frequency (contrasting Fig. 4). [2] Experiment 2 with 20 instead of 5 spikes in the paired spike trains would lead to a *non*-monotonic P_{dis} with respect to frequency (cf. Fig. 5). [3] The full learning curve for trains of 5 spikes versus the time difference of the train onsets would exhibit a maximal up-regulation and maximal down-regulation at -50ms and 100ms , respectively (Fig. 6b). [4] Applying pre- and post-synaptic Poisson spike trains would lead to a monotonic increase of the steady state P_{dis} with respect to the postsynaptic frequency and only to a small decrease with respect to the presynaptic frequency (Fig. 7b). [5] A step change in the frequency of the postsynaptic Poisson spike train after a period of steady state Poisson stimulations would lead to a decrease or increase in P_{dis} depending on the sign of the step change (Fig. 8b). [6] Modulating sinusoidally the frequencies of pre- and post-synaptic Poisson spike trains of lag 0 would lead to an increase in P_{dis} if the modulation frequency is in the range of 1Hz but would not show any change if the modulation rate is faster than 5Hz (Fig. 7). [7] A single presynaptic release followed by a burst of postsynaptic spikes would lead to a superlinear increase of P_{dis} with respect to the burst frequency before eventually saturating.

The last experiment appears to be of particular interest in the light of recently observed Ca^{2+} -triggered bursts in cortical pyramidal cells following coincident apical and somatic stimulations (Larkum et al., 1999). The threshold phenomenon according to which virtually no potentiation is seen for a 1Hz pairing suggests that these bursts are functionally relevant in the present form of synaptic modifications. It also suggests that an incidentally occurring tight pairing would not be able to change the synaptic memory. Finally, more natural stimulation protocols including bursts and Poisson trains would help to specify the activity dependencies of the learning window which is partially expressed in the present data. It would also clarify the question to what extent the same synapse is able to encode individual spike timings while still being sensitive to pre- and post-synaptic average frequencies.

To describe further LTP/LTD experiments one may want to include effects of the post-synaptic membrane potential or the local Ca^{2+} -concentration onto the NMDA-receptor dynamics or the secondary messenger activation. Although we have not examined this, it could easily be achieved by endowing the different rate constants appearing in the scheme with a voltage- or Ca^{2+} -dependent dynamics instead of instantaneously activating them through delta-functions of fixed weights.

Beside the characteristics of strong synaptic depression a large heterogeneity of different synaptic dynamics including facilitation was found between neocortical pyramidal cells (Markram et al., 1998a), suggesting that other parameters governing the temporal response

could be subject to specific learning rules (Markram et al., 1998c). One could speculate that due to additional computation such as the integration of a third coincident signal provided by growth factors or neuromodulators (e.g. synaptic growth or unmasking of postsynaptic receptors (Liao and Malinow, 1995)) is required for the induction of real synaptic strengthening or to gate changes in the recovery time constant. Specifying these conditions remains an important challenge for a future research.

A Appendix

A.1 Differential equations determining the kinetic scheme

For further analysis we give a formulation of the kinetic scheme (Fig. 2) in terms of differential equations. Let us denote by t_{pre}^{rel} the time of a presynaptic release and by t_{post}^{sp} the time of a postsynaptic spike. A presynaptic release at t_{pre}^{rel} will saturate a fraction r_u^N of the recovered NMDA-receptors. A postsynaptic spike at t_{post}^{sp} will block the fraction r_d^N of N_{rec} . The entire dynamics of the NMDA-receptors is:

$$\frac{dN_u}{dt} = -\frac{N_u}{\tau_u^N} + r_u^N N_{rec} \delta(t - t_{pre}^{rel}), \quad (8)$$

$$\frac{dN_d}{dt} = -\frac{N_d}{\tau_d^N} + r_d^N N_{rec} \delta(t - t_{post}^{sp}), \quad (9)$$

$$N_{rec} = 1 - N_d - N_u,$$

where the delta-function $\delta(\dots)$ expresses that the quantities N_u and N_d have to be augmented at the times of a presynaptic release and a postsynaptic spike by $r_u^N N_{rec}$ and $r_d^N N_{rec}$, respectively.

The differential equations for the secondary messengers are:

$$\frac{dS_u}{dt} = -\frac{S_u}{\tau_u^S} + r^S N_u (1 - S_u) \delta(t - t_{post}^{sp}), \quad (10)$$

$$\frac{dS_d}{dt} = -\frac{S_d}{\tau_d^S} + r^S N_d (1 - S_d) \delta(t - t_{pre}^{rel}). \quad (11)$$

The time constants τ_u^S and τ_d^S encompass a diffusion process and are in the range of 300ms. The limit probability is up-regulated at a postsynaptic spike if S_u exceeds some threshold S_u^θ and down-regulated at a presynaptic release if S_d exceeds some threshold S_d^θ . According to the kinetic scheme we have

$$\frac{dP_{dis}^\infty}{dt} = r_u^P (1 - P_{dis}^\infty) [S_u^+ - S_u^\theta]^+ \delta(t - t_{post}^{sp}) - r_d^P P_{dis}^\infty [S_d^+ - S_d^\theta]^+ \delta(t - t_{pre}^{rel}), \quad (12)$$

where S_u^+ and S_d^+ are the values of S_u and S_d immediately after a post- and pre-synaptic spike,

$$S_u^+ = r^S N_u (1 - S_u) + S_u, \quad S_d^+ = r^S N_d (1 - S_d) + S_d. \quad (13)$$

Taking the expectation values in (12) leads to (2). While the changes in P_{dis}^∞ occur instantaneously, the discharge probability P_{dis} slowly approaches the limit probability according to the equation

$$\frac{dP_{dis}}{dt} = \frac{P_{dis}^\infty - P_{dis}}{\tau_M^P}, \quad \text{with} \quad \tau_M^P \approx 10 \text{ min}. \quad (14)$$

A.2 Equations determining the probability of release

A synapse is assumed to have a single site of release from which, according to the univiscular hypothesis, a single vesicle discharges with probability P_{dis} at arrival of a presynaptic spike. Instantaneously after discharge the site of release is empty and it is assumed to be reoccupied by a new vesicle in a Poisson process with time constant $\tau_v^{rec} \approx 800$ ms. The probability P_v that a vesicle is at the site of release is therefore governed by the differential equation

$$\frac{dP_v}{dt} = \frac{1 - P_v}{\tau_v^{rec}} - P_{dis} P_v \delta(t - t_{pre}^{sp}), \quad (15)$$

where t_{pre}^{sp} is the time a presynaptic spike arrives. This equation states that at the time of a presynaptic spike P_v is reset with probability P_{dis} from its actual state back to 0. The probability P_v^{n+1} to encounter a vesicle ready for release at arrival of the $(n+1)$ -th spike is now calculated by

$$P_v^{n+1} = P_v^n (1 - P_{dis}) e^{-\frac{\Delta_n}{\tau}} + (1 - e^{-\frac{\Delta_n}{\tau}}), \quad \tau = \tau_v^{rec}.$$

where $\Delta_n = t_{pre}^{sp, n+1} - t_{pre}^{sp, n}$ is the time elapsed between the two spikes and P_v^n is the probability that a vesicle was ready at the previous spike. Since the probability of release for a presynaptic spike is $P_{rel} = P_{dis} P_v$, we get formula (1). The instantaneous release frequency is calculated from the presynaptic spike frequency according to

$$f_{pre}^{rel} = P_{rel} f_{pre}^{sp} = P_{dis} P_v f_{pre}^{sp}. \quad (16)$$

For presynaptic Poisson spike trains of rate f_{pre}^{sp} one can calculate from (15) the steady state release probability by

$$P_{rel}^{ss} = P_{dis} P_v^{ss} = \frac{P_{dis}}{1 + P_{dis} f_{pre}^{sp} \tau_v^{rec}}.$$

The release frequency at steady state is then given by $f_{pre}^{rel} = P_{rel}^{ss} f_{pre}^{sp}$. Note that due to the memory in the recovery process the release train is not Poissonian anymore.

A.3 Steady state equations for Poisson spike trains

We deduce the steady state of the limit probability of vesicle discharge, $P_{dis}^{\infty, ss}$, for pre- and post-synaptic Poisson spike trains with fixed rates f_{pre}^{sp} and f_{post}^{sp} . Since the time constant τ_M^P for modification is large we may assume that P_{dis} remains constant even during the steady state stimulation. In the following we calculate the steady state value of P_{dis}^{∞} towards which P_{dis} converges after the stimulation according to (14).

First we consider the steady states of the NMDA receptors and the secondary messengers. Replacing the delta-functions in the equations (8-11) with the corresponding rates f_{pre}^{rel} and f_{post}^{sp} we obtain the following expectation value in the steady state,

$$N_u^{ss} = \frac{\rho_u^N f_{pre}^{rel}}{1 + \rho_u^N f_{pre}^{rel} + \rho_d^N f_{post}^{sp}}, \quad \rho_u^N = r_u^N \tau_u^N, \quad (17)$$

$$N_d^{ss} = \frac{\rho_d^N f_{post}^{sp}}{1 + \rho_u^N f_{pre}^{rel} + \rho_d^N f_{post}^{sp}}, \quad \rho_d^N = r_d^N \tau_d^N, \quad (18)$$

$$S_u^{ss} = \frac{\rho_u^S f_{post}^{sp} N_u^{ss}}{1 + \rho_u^S f_{post}^{sp} N_u^{ss}}, \quad \rho_u^S = r_u^S \tau_u^S, \quad (19)$$

$$S_d^{ss} = \frac{\rho_d^S f_{pre}^{rel} N_d^{ss}}{1 + \rho_d^S f_{pre}^{rel} N_d^{ss}}, \quad \rho_d^S = r_d^S \tau_d^S. \quad (20)$$

Note that due to the shared pool N_{rec} the variables N_x and S_x ($x = u, d$) are not independent and that, strictly speaking, we are not allowed to average the product in (10) and (11) individually. However, as long as one of the frequencies f_{post}^{sp} and f_{pre}^{rel} is small compared to the time constants τ_x^N and τ_x^S , one of the variables N_x and S_x has always time to relax towards its mean between the jumps of the other. Indeed, for $\tau_v^{rec} \approx 1$ the release rate will be less than ≈ 1 Hz while the time constants in consideration are all smaller than $\approx .5$ seconds and formulas (19) and (20) turn out to be a good approximation (cf. Fig. 7a). Also, the error we are handling in by treating f_{pre}^{rel} as a Poisson rate seems to be marginal. By a similar reasoning we may average the individual factors in Eq. (12) to obtain

$$0 = r_u^P (1 - P_{dis}^{\infty ss}) [S_u^+ - S_u^\theta]^{+ss} f_{post}^{sp} - r_d^P P_{dis}^{\infty ss} [S_u^+ - S_u^\theta]^{+ss} f_{pre}^{rel}, \quad (21)$$

where again the superscript ss denotes the expectation value of the corresponding quantity in the steady state. If the variation of S_x is small the quantity $[S_x^+ - S_x^\theta]^{+ss}$ can be approximated by $[S_x^{+ss} - S_x^\theta]^+$ and in case of vanishing thresholds $S_x^\theta = 0$ it is equal to

$$S_x^{+ss} = r^S N_x^{ss} (1 - S_x^{ss}) + S_x^{ss}, \quad x \in \{u, d\}. \quad (22)$$

In this case one obtains from (21) the expectation value of P_{dis}^{∞} in the steady state,

$$P_{dis}^{\infty ss} = \frac{1}{1 + \frac{r_d^P f_{pre}^{rel} S_d^{+ss}}{r_u^P f_{post}^{sp} S_u^{+ss}}}, \quad (23)$$

which in general is a good approximation if S_x^+ is most of the time above the threshold S_x^θ .

It is elusive to study the transition from the full model to the reduced model which just considers the cross-gating of the NMDA receptors without secondary messengers. From (12) we get at steady state with vanishing thresholds

$$\frac{dP_{dis}^{\infty}}{dt} = r_u^P (1 - P_{dis}^{\infty ss}) S_u^{+ss} f_{pos}^{sp} - r_d^P P_{dis}^{\infty ss} S_d^{+ss} f_{pre}^{rel}. \quad (24)$$

Linearizing N_x^{ss} and S_x^{ss} (17-20) around zero frequencies (thereby neglecting saturation effects) and inserting into (22) yields

$$S_u^{+ss} \approx \tilde{\rho}_u^N f_{pre}^{rel} (1 - \tilde{\rho}_u^S \tau_u^S f_{pos}^{sp} f_{pre}^{rel}) + \tilde{\rho}_u^S \tau_u^S f_{pos}^{sp} f_{pre}^{rel} \quad (25)$$

$$S_d^{+ss} \approx \tilde{\rho}_d^N f_{pre}^{rel} (1 - \tilde{\rho}_d^S \tau_d^S f_{pre}^{rel} f_{post}^{sp}) + \tilde{\rho}_d^S \tau_d^S f_{pre}^{rel} f_{post}^{sp}, \quad (26)$$

with appropriate constants $\tilde{\rho}_x^X$. If $\tau_u^S f_{pos}^{sp}$ and $\tau_d^S f_{pre}^{rel}$ is small, the second term in (25, 26) vanishes, and the synaptic change is dominated by the 2nd order correlations,

$$\frac{dP_{dis}^{\infty}}{dt} \approx \tilde{r}_u^P (1 - P_{dis}^{\infty ss}) f_{pre}^{rel} f_{pos}^{sp} - \tilde{r}_d^P P_{dis}^{\infty ss} f_{post}^{sp} f_{pre}^{rel}.$$

This is in particular true if $\tau^S = 0$ (and the secondary messengers therefore only act by a constant factor). If on the other hand $\tau_u^S f_{pos}^{sp}$ and $\tau_d^S f_{pre}^{rel}$ is large, the secondary messengers are closer to saturation ($S_x^{ss} \approx 1$), the second term in (25, 26) is now dominating, and a 3rd order correlation enters in (24). This reasoning also motivates the short forms (6) and (7) of the learning rule for the non-steady state situation and the cases $\tau^S = 0$ and $\tau^S > 1/f$, respectively.

A.4 Deduction of the BCM properties

To show the connection to the BCM theory (Bienenstock et al., 1982) we assume $S_d^0 = 0$ and consider our learning rule (2). Inserting the parameters into Eq. 12 shows that the time constant of P_{dis}^∞ is of an order slower than that of S_u and S_d (cf. Figs 7a and 8a). In the limit of slow adaptation of P_{dis}^∞ we may thus replace the quantities S_u^+ and S_d^+ by their steady state values. Writing the learning rule in the form (3) we obtain

$$\phi(f_{post}^{sp}) = (1 - P_{dis}^\infty) [S_u^{+ss} - S_u^\theta]^+ \frac{f_{post}^{sp}}{f_{pre}^{rel}} - \frac{r_d^P}{r_u^P} P_{dis}^\infty S_d^{+ss}. \quad (27)$$

We have to show that this function satisfies the requirements of the BCM learning curves. The first requirement $\phi(0) = 0$ is readily checked since S_d^{+ss} vanishes for $f_{post}^{sp} = 0$ according to (18) and (20). We have $\phi'(0) < 0$ since for small f_{post}^{sp} the second term in (27) will dominate for $r_d^P > 0$. This is true since the first term is bound from above by $(f_{post}^{sp})^2$ and the second term is bound from below by f_{post}^{sp} . Since for large f_{post}^{sp} it is the first term in (27) which dominates we get a second zero of ϕ at

$$\theta_M = \frac{r_d^P}{r_u^P} \frac{P_{dis}^\infty}{1 - P_{dis}^\infty} \frac{S_d^{+ss}}{[S_u^{+ss} - S_u^\theta]^+} f_{pre}^{rel} \quad (28)$$

with $\phi'(\theta_M) \geq 0$. The modification threshold is implicitly driven by the postsynaptic spike rate f_{post}^{sp} which changes S_u^{+ss} and S_d^{+ss} via (17)-(20) and this in turn changes P_{dis}^∞ via learning rule (3). The convergence of P_{dis}^∞ for fixed frequencies ensures that eventually the RHS of (3) vanishes and this, by definition, happens when $\theta_M = f_{post}^{sp}$. For example, if f_{post}^{sp} grows over θ_M , we have $\phi(f_{post}^{sp}) > 0$ and the learning rule pushes P_{dis}^∞ up. Due to the factor $P_{dis}^\infty/(1 - P_{dis}^\infty)$, however, the threshold θ_M increases as well. Since the speed of θ_M is nonlinear in P_{dis}^∞ this factor dominates the (saturating) changes in S_u^{+ss} and S_d^{+ss} . The threshold θ_M will therefore eventually catch up and overtake f_{post}^{sp} and we get $\phi(f_{post}^{sp}) < 0$. According to the learning rule, P_{dis}^∞ now starts to decrease again. Hence, Eq. (28) incorporates the sliding threshold property with respect to f_{post}^{sp} and this keeps the synapse sensitive to its environment.

A.5 Change of P_{dis}^∞ for nonzero spike correlations

We first quantify the effect of the spike correlation onto the distribution of the up- and down-regulating quantities N_u and N_d in their steady states. Recall that for a spike correlation of e.g. $c_s = 1$ each postsynaptic spike follows instantaneously after a presynaptic spike. For a positive spike correlation $c_s \in [0, 1]$, the effective postsynaptic frequency is reduced by the fraction $r_u^N [c_s]^+ P_{rel}^{ss}$ and we must replace f_{post}^{sp} by $(1 - r_u^N [c_s]^+ P_{rel}^{ss}) f_{post}^{sp}$ in the formulas (17, 18) giving the average values of N_u and N_d , respectively. Similarly, for a negative spike correlation $c_s \in [-1, 0]$ the presynaptic release frequency f_{pre}^{rel} must be replaced by $(1 - r_d^N [-c_s]^+) f_{pre}^{rel}$ in the same two formulas, and the steady states N_u^{ss} and N_d^{ss} become functions of c_s . Next, in the formulas (19,20,22) the quantities N_u^{ss} and N_d^{ss} have to be replaced by their average values immediately after a pre- or post-synaptic spike, i.e. by $N_u^{ss+} = N_u^{ss} + r_u^N [c_s]^+ P_{rel}^{ss} N_{rec}^{ss}$ and $N_d^{ss+} = N_d^{ss} + r_d^N [-c_s]^+ N_{rec}^{ss}$, respectively. (Since due to the memory in the vesicle recovery process the presynaptic release train is not Poissonian, we would not be allowed to replace the delta-function by the release rate to calculate the mean-field behavior. If in addition there is a non-vanishing correlation between the pre- and postsynaptic spike trains this ‘simplification’ indeed cannot be neglected anymore

and we were urged to empirically correct the mean-field plots in Fig. 10 by a factor of 1.3 in front of c_s .) If we now put $S_u^\theta = S_d^\theta = 0$ we get from (21) the steady state of P_{dis}^∞ as a function of the spike correlation c_s (cf. Fig. 10b). The mean-field evolution of P_{dis}^∞ for a given spike correlation $c_s \in [-1, 1]$ is obtained by the analog replacements (while dropping the upper index ss) in the formulas (8)-(11) and (13).

Acknowledgments

This study was supported by the Priority Program Biotechnology of the Swiss National Fund (grant 5002-44893) (WS), the Office of Naval Research, the Human Frontier Science Program Organization and the Israeli Academy of Sciences (HM and MT);

References

- Abbott, L. (1996). Decoding Neuronal Firing and Modeling Neural Networks. *Quart. Rev. Biophys.*, 27:291–331.
- Abbott, L. & Song, S. (1999). Temporally Asymmetric Hebbian Learning, Spike Timing and Neuronal Response Variability. In: *Advances in Neural Information Processing Systems*, M. Kearns, S. Solla, & D. Cohn, ed., volume 11. MIT Press, Cambridge MA.
- Abbott, L., Varela, J., Sen, K., & Nelson, S. (1997). Synaptic Depression and Cortical Gain Control. *Science*, 275:220–224.
- Antonov, S., Gmiro, V., & Johnson, J. (1998). Binding sites for permeant ions in the channel of NMDA receptors and their effects on channel block. *nature neuroscience*, 1(6):451–461.
- Artola, A. & Singer, W. (1993). Long-term depression of excitatory synaptic transmission and its relationship to long-term potentiation. *Trends in Neurosci.*, 16(11):480–487.
- Bear, M., Cooper, L. N., & Ebner, F. F. (1987). A Physiological Basis for a Theory of Synapse Modification. *Science*, 237:42–48.
- Bell, C., Han, V., Sugawara, Y., & Grant, K. (1997). Synaptic plasticity in a cerebellum-like structure depends on temporal order. *Nature*, 387 (6630):278–281.
- Bi, Q. & Poo, M. (1998). Precise spike timing determines the direction and extent of synaptic modifications in cultured hippocampal neurons. *J. Neurosci.*, 18:10464–10472.
- Bienenstock, E., Cooper, L., & Munro, P. (1982). Theory for the development of neuron selectivity: orientation specificity and binocular interaction in visual cortex. *J. Neurosci.*, 2(1):32–48.
- Blum, K. & Abbott, L. (1996). A model of spatial map formation in the hippocampus of the rat. *Neural Computation*, 8(1):85–93.
- Brown, T. H. & Chatterji, S. (1994). Hebbian Synaptic Plasticity: Evolution of the Contemporary Concept. In: *Model of neural networks II*, E. Domany, J. van Hemmen, & K. Schulten, ed., chapter 8, pages 287–314. Springer.
- Debanne, D., Shulz, D., & Fregnac, Y. (1995). Temporal constraints in associative synaptic plasticity in hippocampus and neocortex. *Can. J. Physiol. and Pharmacol.*, 73:1295–1311.
- Fregnac, Y. & Shulz, D. (1994). Models of synaptic plasticity and cellular analogs of learning in the developing and adult visual cortex. In: *Advances in Neural and Behavioral Development*, V. Casagrande & P. Shinkman, ed., (4 ed.). Ablex Publ. Corp., Norwood, New Jersey.
- Fregnac, Y., Shulz, D., Thorpe, S., & Bienenstock, E. (1988). A cellular analogue of visual cortical plasticity. *Nature*, 333:367–370.
- Fusi, S., Annunziato, M., Badoni, D., Salamon, A., & D.J.Amit (1999). Spike-driven synaptic plasticity: theory, simulation, VLSI implementation. *Neural Computation*. submitted.
- Gerstner, W. & Abbott, L. (1997). Learning navigational maps through potentiation and modulation of hippocampal place cells. *J. Comput. Neuroscience*, 4:79–94.
- Gerstner, W., Kempter, R., van Hemmen, J., & Wagner, H. (1996). A neuronal learning rule for sub-millisecond temporal coding. *Nature*, 383:76–78.
- Gerstner, W., Kempter, R., van Hemmen, J., & Wagner, H. (1998). Hebbian learning of pulse timing in the barn owl auditory system. In: *Pulsed Neural Networks*, W. Maass & C. Bishop, ed., chapter 14. MIT press.

- Grzywacz, N. & Burgi, P.-Y. (1998). Toward a Biophysically Plausible Bidirectional Hebbian Rule. *Neural Computation*, 10:499–520.
- Gustafsson, B., Wigström, H., Abraham, W., & Huang, Y.-Y. (1987). Long-Term Potentiation in the Hippocampus Using Depolarizing Current Pulses as the Conditioning Stimulus to Single Volley Synaptic Potentials. *J. Neurosci.*, 7:774–780.
- Hebb, D. O. (1949). *The Organization of Behaviour*. Wiley and Sons, New York.
- Hopfield, J. (1995). Pattern recognition computation using action potential timing for stimulus representation. *Nature*, 376:33–36.
- Jonas, P. & Spruston, N. (1994). Mechanisms shaping glutamate-mediated excitatory postsynaptic currents in the CNS. *Curr. Opin. Neurobiol.*, 4(3):366–372.
- Kempter, R., Gerstner, W., & van Hemmen, J. (1999a). Hebbian learning and spiking neurons. *Physical Review E*, 59(4):4498–4514.
- Kempter, R., Gerstner, W., & van Hemmen, J. (1999b). Spike-based Compared to Rate-based Hebbian Learning. In: *Advances in Neural Information Processing Systems 11*, S. S. et al., ed., page in press.
- Larkum, M., Zhu, J., & Sakmann, B. (1999). A novel cellular mechanism for coupling inputs arriving at different cortical layers. *Nature*, 398:338–341.
- Liao, D. & Malinow, N. H. R. (1995). Activation of postsynaptically silent synapses during pairing-induced LTP in CA1 region of hippocampal slice. *Nature*, 375:400–404.
- Maass, W. (1998). A simple model for neural computation with firing rates and firing correlations. *Network: Computation in Neural Systems*, 9(3):381–397.
- Markram, H., Helm, P., & Sakmann, B. (1995). Dendritic calcium transients evoked by single back-propagating action potentials in rat neocortical pyramidal neurons. *J. Physiol. (London)*, 485:1–20.
- Markram, H., Lübke, J., Frotscher, M., & Sakmann, B. (1997). Regulation of Synaptic Efficacy by Coincidence of Postsynaptic APs and EPSPs. *Science*, 275:213–215.
- Markram, H., Pikus, D., Gupta, A., & Tsodyks, M. (1998a). Potential for multiple mechanisms, phenomena and algorithms for synaptic plasticity at single synapses. *Neuropharmacology*, 37:489–500.
- Markram, H., Roth, A., & Helmchen, F. (1998b). Competitive calcium binding: implications for dendritic calcium signaling. *JCNS*, 5 (3):331–348.
- Markram, H. & Tsodyks, M. (1996). Redistribution of synaptic efficacy between neocortical pyramidal neurons. *Nature*, 382:807–810.
- Markram, H., Wang, Y., & Tsodyks, M. (1998c). Differential synaptic transmission via the same axon from neocortical layer 5 pyramidal neurons. *PNAS*, pages 5323–5328.
- Mayer, M. (1998). Ion-binding sites in NMDA receptors: classical approaches provide the numbers. *nature neuroscience*, 1(6):433–434.
- Mayer, M., McDermott, A., Westbrook, G., Smith, S., & Barker, J. (1987). Agonist- and Voltage-Gated Calcium Entry in Cultured Mouse Spinal Cord Neurons Under Voltage Clamp Measured Using Arsenazo III. *J. Neurosci.*, 7:3230–3244.
- Medina, I., Filippova, N., Bakhramov, A., & Bregestovski, P. (1996). Calcium-induced inactivation of NMDA receptor-channels evolves independently of run-down in cultured rat brain neurones. *J. Physiol. (London)*, 495:411–427.
- Oja, E. (1982). A simplified neuron model as a principal component analyzer. *J. Math. Biol.*, 15:267–273.
- Sejnowski, T. (1977). Storing Covariance With Nonlinearly Interacting Neurons. *J. Math. Biol.*, 4:303–321.
- Senn, W., Tsodyks, M., & Markram, H. (1997). An algorithm for synaptic modification based on exact timing of pre-and post-synaptic action potentials. In: *Artificial Neural Networks - ICANN'97*, W. Gerstner, A. Germond, M. Hasler, & J.-D. Nicoud, ed., volume 1327 of *Lecture Notes in Computer Science*, pages 121–126.
- Spruston, N., Jonas, P., & Sakmann, B. (1995). Dendritic glutamate receptor channels in rat hippocampal CA3 and CA1 pyramidal neurons. *J. Physiol. (London)*, 482:325–352.
- Stanton, P. & Sejnowski, T. (1989). Associative long-term depression in the hippocampus induced

- by hebbian covariance. *Nature*, 339:215–218.
- Triller, A. & Korn, H. (1982). Transmission at a central inhibitory synapse. III Ultrastructure of physiologically identified and stained terminals. *J. Neurophysiol.*, 48:708–736.
- Tsodyks, M. & Markram, H. (1997). The neural code between neocortical pyramidal neurons depends on neurotransmitter release probability. *Proc. Natl. Acad. Sci. USA*, 94:719–723.
- Tsumoto, T. (1990). Long-term potentiation and depression in the cerebral neocortex. *Jpn. J. Physiol.*, 40:573–593.
- Zhang, L., Tao, H., Holt, C., Harris, W., & Poo, M. (1998). A critical window in the cooperation and competition among developing retinotectal synapses. *Nature*, 395:37–44.